



# Airborne intercomparison of HO<sub>x</sub> measurements using laser-induced fluorescence and chemical ionization mass spectrometry during ARCTAS

X. Ren<sup>1</sup>, J. Mao<sup>2</sup>, W. H. Brune<sup>3</sup>, C. A. Cantrell<sup>4</sup>, R. L. Mauldin III<sup>4,\*</sup>, R. S. Hornbrook<sup>4</sup>, E. Kosciuch<sup>4</sup>, J. R. Olson<sup>5</sup>, J. H. Crawford<sup>5</sup>, G. Chen<sup>5</sup>, and H. B. Singh<sup>6</sup>

<sup>1</sup>Air Resources Laboratory, National Oceanic and Atmospheric Administration, Silver Spring, Maryland, USA

<sup>2</sup>Geophysical Fluid Dynamics Laboratory, National Oceanic and Atmospheric Administration, Princeton, New Jersey, USA

<sup>3</sup>Department of Meteorology, Pennsylvania State University, University Park, Pennsylvania, USA

<sup>4</sup>Atmospheric Chemistry Division, National Center for Atmospheric Research, Boulder, Colorado, USA

<sup>5</sup>Science Directorate, NASA Langley Research Center, Hampton, Virginia, USA

<sup>6</sup>Earth Science Division, NASA Ames Research Center, Moffett Field, California, USA

\* now at: University of Helsinki, Helsinki, Finland and University of Colorado, Boulder, CO, USA

Correspondence to: X. Ren (xinrong.ren@noaa.gov)

Received: 2 March 2012 – Published in Atmos. Meas. Tech. Discuss.: 30 March 2012

Revised: 24 July 2012 – Accepted: 25 July 2012 – Published: 21 August 2012

**Abstract.** The hydroxyl (OH) and hydroperoxyl (HO<sub>2</sub>) radicals, collectively called HO<sub>x</sub>, play central roles in tropospheric chemistry. Accurate measurements of OH and HO<sub>2</sub> are critical to examine our understanding of atmospheric chemistry. Intercomparisons of different techniques for detecting OH and HO<sub>2</sub> are vital to evaluate their measurement capabilities. Three instruments that measured OH and/or HO<sub>2</sub> radicals were deployed on the NASA DC-8 aircraft throughout Arctic Research of the Composition of the Troposphere from Aircraft and Satellites (ARCTAS) in the spring and summer of 2008. One instrument was the Penn State Airborne Tropospheric Hydrogen Oxides Sensor (ATHOS) for OH and HO<sub>2</sub> measurements based on Laser-Induced Fluorescence (LIF) spectroscopy. A second instrument was the NCAR Selected-Ion Chemical Ionization Mass Spectrometer (SI-CIMS) for OH measurement. A third instrument was the NCAR Peroxy Radical Chemical Ionization Mass Spectrometer (PeRCIMS) for HO<sub>2</sub> measurement. Formal intercomparison of LIF and CIMS was conducted for the first time on a same aircraft platform. The three instruments were calibrated by quantitative photolysis of water vapor by ultraviolet (UV) light at 184.9 nm with three different calibration systems. The absolute accuracies were ±32 % (2σ) for the LIF instrument, ±65 % (2σ) for the SI-CIMS instrument, and ±50 %

(2σ) for the PeRCIMS instrument. In general, good agreement was obtained between the CIMS and LIF measurements of both OH and HO<sub>2</sub> measurements. Linear regression of the entire data set yields  $[\text{OH}]_{\text{CIMS}} = 0.89 \times [\text{OH}]_{\text{LIF}} + 2.8 \times 10^4 \text{ cm}^{-3}$  with a correlation coefficient  $r^2 = 0.72$  for OH, and  $[\text{HO}_2]_{\text{CIMS}} = 0.86 \times [\text{HO}_2]_{\text{LIF}} + 3.9$  parts per trillion by volume (pptv, equivalent to  $\text{pmol mol}^{-1}$ ) with a correlation coefficient  $r^2 = 0.72$  for HO<sub>2</sub>. In general, the difference between CIMS and LIF instruments for OH and HO<sub>2</sub> measurements can be explained by their combined measurement uncertainties. Comparison with box model results shows some similarities for both the CIMS and LIF measurements. First, the observed-to-modeled HO<sub>2</sub> ratio increases greatly for higher NO mixing ratios, indicating that the model may not properly account for HO<sub>x</sub> sources that correlate with NO. Second, the observed-to-modeled OH ratio increases with increasing isoprene mixing ratios, suggesting either incomplete understanding of isoprene chemistry in the model or interferences in the measurements in environments where biogenic emissions dominate ambient volatile organic compounds.

## 1 Introduction

The hydroxyl radical (OH) is the primary oxidizing species in the troposphere and reacts with most natural and anthropogenic trace gases emitted into the atmosphere, thereby initiating their oxidation and final removal from the atmosphere (Logan et al., 1981; Ehhalt et al., 1991; Lelieveld et al., 2004). The hydroperoxyl radical (HO<sub>2</sub>) is an important ozone precursor through its reaction with NO. The chemistry of OH and HO<sub>2</sub> (OH and HO<sub>2</sub> are collectively called HO<sub>x</sub>) impacts many environmental issues such as ozone and fine particle formation. Because of the important roles OH and HO<sub>2</sub> play in atmospheric chemistry, it has been a high priority that OH and HO<sub>2</sub> are accurately measured.

Three techniques have been widely used for tropospheric OH measurements, including Laser-Induced Fluorescence (LIF, also known as FAGE – Fluorescence Assay with Gas Expansion) spectroscopy (Hard et al., 1984; Stevens et al., 1994; Holland et al., 1995; Heal et al., 1995; Kanaya et al., 2001; Dusanter et al., 2008; Martinez et al., 2010; Commane et al., 2010), Chemical Ionization Mass Spectrometry (CIMS) (Eisele and Tanner, 1991; Berresheim et al., 2000), and Differential Optical Laser Absorption Spectroscopy (DOAS) (Perner et al., 1976; Armerding et al., 1994; Mount et al., 1997). Over the past 15–20 yr, the sensitivity and time resolution have been significantly improved for OH measurements by LIF and CIMS, although the absolute calibrations still have relatively large uncertainties. DOAS has been used as a reference method with no calibration needed but, with a relatively long time resolution of ~ 100 s and detection limit of ~ 1 × 10<sup>6</sup> molecules cm<sup>-3</sup>, it has had limited use in field studies.

Since the mid 1990s, HO<sub>2</sub> has been successfully measured by LIF as OH after the conversion of HO<sub>2</sub> by NO (Brune et al., 1995; Mather et al., 1997). Lately, CIMS OH instruments were adapted to measure HO<sub>2</sub> and organic peroxy radicals (RO<sub>2</sub>) by amplified conversion to H<sub>2</sub>SO<sub>4</sub> via OH in a chain reaction with added NO and SO<sub>2</sub> and using controlled ratios of NO/O<sub>2</sub>, e.g., the RO<sub>x</sub> Chemical Conversion/CIMS (ROX-MAS) (Hanke et al., 2002) and the Peroxy Radical Chemical Ionization Mass Spectrometer (PeRCIMS) (Edwards et al., 2003; Hornbrook et al., 2011).

Deployments of LIF and CIMS for OH and HO<sub>2</sub> measurements in ground-based field campaigns and on mobile platforms have significantly improved our understanding of HO<sub>x</sub> chemistry and have also indicated gaps in our current knowledge. For instance, in areas strongly influenced by biogenic emissions with low NO<sub>x</sub> mixing ratios, measured OH amounts were found to be significantly higher than modeled values (e.g., Faloon et al., 2001; Tan et al., 2001; Di Carlo et al., 2004; Ren et al., 2008; Lelieveld et al., 2008; Hofzumahaus et al., 2009; Petäjä et al., 2009; Martinez et al., 2010; Whalley et al., 2011; Lu et al., 2012;). In high NO<sub>x</sub> environments, models typically underestimate HO<sub>2</sub> measurements (e.g., Ren et al., 2005, 2008; Kanaya et al., 2012; Lu et al.,

2012). These discrepancies imply either fundamental flaws in current understanding of tropospheric HO<sub>x</sub> chemistry or measurement errors.

A recent study by Fuchs et al. (2011) found that previous measurements of HO<sub>2</sub> with LIF might be biased by interference from RO<sub>2</sub> radicals that are produced in the oxidation of alkenes (including isoprene) and aromatics. In another study conducted in a California forest where biogenic emissions dominate, a new chemical removal method was deployed to measure OH in parallel to the traditional FAGE method with wavelength modulation. This new method shows significantly lower OH signal compared to the traditional method (Mao et al., 2012). Because of considerable uncertainties associated with calibration and possible instrument errors, intercomparisons of different HO<sub>x</sub> measurement techniques are thus crucial to achieve high-quality measurement data and reduce instrument uncertainties.

Several HO<sub>x</sub> intercomparison studies have been conducted in the past 20 yr or so, mostly in ground-based campaigns (e.g., Eisele et al., 1994; Campbell et al., 1995; Brauers et al., 1996; Mount et al., 1997; Hofzumahaus et al., 1998; Schlosser et al., 2007). These intercomparisons of tropospheric OH measurements have been reviewed by Schlosser et al. (2009). During the HO<sub>x</sub>Comp campaign in 2005, one DOAS, one CIMS, and four LIF instruments were compared formally, sampling both ambient air and the atmospheric chamber SAPHIR in Jülich, Germany. All instruments measured tropospheric OH concentrations with good sensitivity and time resolution. Sampling inhomogeneities and calibration uncertainties were given as the explanations for the discrepancies in the ambient measurements (Schlosser et al., 2009). During HO<sub>x</sub>Comp, three LIF instruments also measured HO<sub>2</sub> in both ambient and chamber air. Measurements from these LIF instruments were well correlated, and the discrepancies were likely related to interference from water vapor and ozone in the chamber measurements and sampling inhomogeneities in the ambient measurements (Fuchs et al., 2010; Kanaya et al., 2012). In 2007, a comparison was conducted between a Matrix Isolation Electron Spin Resonance (MIESR) instrument and an LIF instrument (ROxLIF) capable of detecting HO<sub>2</sub> and the sum of organic peroxy radicals (RO<sub>2</sub>) during two experiments in the SAPHIR chamber. Measurements of HO<sub>2</sub> agreed on average to within 5 % (Fuchs et al., 2009). In an earlier HO<sub>2</sub> intercomparison study, a PeRCIMS and an LIF instrument were compared for HO<sub>2</sub> measurement in two phases: (1) by mutual exchange of calibration sources, and (2) by ambient air measurements (Ren et al., 2003). Good correlation was found in both phases. However, the LIF-measured HO<sub>2</sub> was higher than the CIMS-measured HO<sub>2</sub> by a factor of 1.6 after considering a calibration change in the LIF instrument that was discovered later (Ren et al., 2008; Mao et al., 2010).

Airborne OH and HO<sub>2</sub> measurements have been compared for instruments on different aircraft flying in close formation (Eisele et al., 2001, 2003; Kleb et al., 2011). During

the Pacific Exploratory Mission Tropics B (PEM-TB) study in 1999, LIF OH measurements on the NASA DC-8 and CIMS OH measurements on the NASA P-3B aircraft showed excellent agreement in the marine boundary layer with an average measurement difference similar to the uncertainty of each technique ( $\sim \pm 40\%$ ,  $2\sigma$  uncertainty). The ratio of LIF-to-CIMS OH increased from 0.8 near the surface to 1.6 at 8-km altitude (Eisele et al., 2001). During the Transport and Chemical Evolution over the Pacific (TRACE-P) campaign in 2001, excellent agreement was again obtained between the LIF and CIMS OH measurements, with a slope of 0.96 and a correlation coefficient ( $r^2$ ) of 0.88, after considering the revised values for the LIF OH measurements by a factor of 1.6 higher due to a calibration error discovered later (Ren et al., 2008). The Intercontinental Chemical Transport Experiment-B (INTEX-B) campaign in 2006 involved three 40–60 min comparison periods with the Penn State LIF instrument measuring OH and HO<sub>2</sub> on the NASA DC-8 and two NCAR CIMS instruments measuring OH and HO<sub>2</sub>/HO<sub>2</sub>+RO<sub>2</sub>, respectively, on the NSF C-130. The median CIMS HO<sub>2</sub> to LIF HO<sub>2</sub> ratio was 1.23 with a correlation coefficient ( $r^2$ ) of 0.59. The median CIMS OH to LIF OH ratio was 0.81, but surprisingly with very little correlation ( $r^2 = 0.03$ ) (Kleb et al., 2011). This low correlation is mainly due to low quality CIMS OH data in one of the three intercomparison flights that were used. Thus intercomparisons of HO<sub>x</sub> measurements on different aircraft have been inconclusive, possibly because the instruments were not consistently sampling the same air mass or because small fluctuations in instrument performance could be occurring in the limited intercomparison periods. Deploying different HO<sub>x</sub> instruments on one aircraft solves both of these problems and provides a more rigorous and definitive comparison.

In this study, we present a formal intercomparison of OH and HO<sub>2</sub> measurements performed by three different instruments aboard the NASA DC-8 aircraft during the Arctic Research of the Composition of the Troposphere from Aircraft and Satellites (ARCTAS) campaign. The three instruments were the Penn State Airborne Tropospheric Hydrogen Oxides Sensor (ATHOS) for OH and HO<sub>2</sub> measurements based on LIF spectroscopy, the NCAR Selected-Ion Chemical Ionization Mass Spectrometer (SI-CIMS) for OH measurement, and the NCAR Peroxy Radical Chemical Ionization Mass Spectrometer (PeRCIMS) for HO<sub>2</sub> measurement. These measurements were also compared to box model results to investigate similarities and differences in both CIMS and LIF measurements.

## 2 Experimental description

### 2.1 ARCTAS mission

The NASA ARCTAS mission was conducted in two 3-week deployments based in Alaska (April 2008, ARCTAS-A) and

western Canada (June–July 2008, ARCTAS-B). Its objective was to better understand the factors driving current changes in Arctic atmospheric composition and climate. Details of the background, design, execution, and components of ARCTAS can be found in Jacob et al. (2010). The ARCTAS-B deployment was preceded by one week of flights over California sponsored by the California Air Resources Board (ARCTAS-CARB) to improve state emission inventories for greenhouse gases and aerosols and to provide observations to test and improve models of ozone and aerosol pollution. For the purpose of comparing HO<sub>x</sub> measurement under a variety of conditions, in particular those with high NO<sub>x</sub> and VOC levels, HO<sub>x</sub> measurements during ARCTAS-CARB were included in the intercomparison.

### 2.2 LIF HO<sub>x</sub> instrument

OH and HO<sub>2</sub> radicals were measured with the Penn State ATHOS instrument. ATHOS detects OH and HO<sub>2</sub> with LIF spectroscopy. The technique uses a pump-down technique often called the fluorescent assay by gas expansion (FAGE) originally developed by Hard et al. (1984). A detailed description of the ATHOS instrument can be found in Faloon et al. (2004); here, an abbreviated description of ATHOS is given.

Sample air is drawn into a low-pressure chamber through a pinhole inlet (1.5 mm) with a vacuum pump. The pressure of the detection chamber varies from 12 to 3 hPa from 0- to 12-km altitude, respectively. As the air passes through a laser beam, OH is excited by a spectrally narrowed laser with a pulse repetition rate of 3 kHz at one of several ro-vibronic transition lines near 308 nm ( $A^2\Sigma - X^2\Pi$ ,  $v' = 0 \leftarrow v'' = 0$ ). Collisional quenching of the excited state of OH is slow enough at the chamber pressure that the weak OH fluorescence extends beyond the prompt scattering (Rayleigh and wall scattering) and is detected with a time-gated microchannel plate (MCP) detector. HO<sub>2</sub> is measured by its reaction with NO followed by LIF detection of OH. The OH and HO<sub>2</sub> detection axes are in series: OH is detected in the first axis and HO<sub>2</sub> in a second axis as reagent NO (> 99%, Matheson, Twinsburg, Ohio, purified through Ascarite sodium hydroxide) is added to the flow between the two axes. The OH fluorescence signal is detected 60 ns after the laser pulse has cleared in the detection cells and is recorded every 0.2 s. The laser wavelength is tuned on-resonance with an OH transition for 15 s and off-resonance for 5 s, resulting in a measurement time resolution of 20 s. The OH fluorescence signal is the difference between on-resonance and off-resonance signals.

The instrument was calibrated on the ground both in the laboratory and during the field campaign. Different sizes of pinholes were used in the calibration to produce different detection cell pressures. Laboratory and in-situ flight tests indicated that OH and HO<sub>2</sub> loss from the pinhole is negligible (Faloon et al., 2004). Monitoring laser power, Rayleigh scattering, and laser linewidth maintained this calibration in

flight (Faloona et al., 2004). For the calibration, OH and HO<sub>2</sub> were produced through water vapor photolysis by ultraviolet (UV) light at 184.9 nm. Absolute OH and HO<sub>2</sub> mixing ratios were calculated by knowing the 184.9 nm photon flux, which was determined with a CsI phototube referenced to a NIST-calibrated photomultiplier tube, the H<sub>2</sub>O absorption cross section, the H<sub>2</sub>O mixing ratio, and the exposure time of the H<sub>2</sub>O to the 184.9 nm light. The absolute uncertainty was estimated to be  $\pm 32\%$  for both OH and HO<sub>2</sub> at a  $2\sigma$  confidence level. The  $2\sigma$  precision for a 1-minute integration time during this campaign was about 0.01 parts per trillion by volume (pptv, equivalent to pmol mol<sup>-1</sup>) for OH and 0.1 pptv for HO<sub>2</sub>. Further details about the calibration process may be found in Faloona et al. (2004).

A recent laboratory study suggests that the HO<sub>2</sub> measurements in some FAGE-type instruments are susceptible to interference from RO<sub>2</sub> species arising from the oxidation of alkenes and aromatics (Fuchs et al., 2011). A laboratory study showed that ATHOS is also affected by this interference. Compared to HO<sub>2</sub>, the relative detection sensitivities of RO<sub>2</sub> are 0.68 for isoprene, 0.66 for ethene, 0.40 for cyclohexane, and 0.54 for  $\alpha$ -pinene. Determination of sensitivities from additional alkenes and aromatics is still needed, but a mean sensitivity of  $0.60 \pm 0.15$  is consistent with all species that have been measured to date. Measured HO<sub>2</sub> was thus corrected by 0.6 times RO<sub>2</sub> (modeled) initiated from alkenes plus aromatics. Due to relatively low alkene and aromatic mixing ratios during ARCTAS, this correction reflects only a decrease of HO<sub>2</sub> by 4% on average.

During ARCTAS, the ATHOS nacelle inlet was mounted below a nadir plate of the forward cargo bay of the DC-8 while the lasers, electronics, and vacuum pump were housed inside the forward cargo bay (Fig. 1).

### 2.3 CIMS OH instrument

The NCAR SI-CIMS instrument uses chemical conversion of ambient OH with <sup>34</sup>SO<sub>2</sub> to produce H<sub>2</sub><sup>34</sup>SO<sub>4</sub>, which subsequently reacts with NO<sub>3</sub><sup>-</sup> reactant ions to produce H<sup>34</sup>SO<sub>4</sub><sup>-</sup> that is detected by a mass spectrometer. The system consists of four major sections: a shrouded inlet that straightens and slows the air flow, a chemical reaction region in which the neutral chemistry takes place, an ion reaction region in which the chemical ionization reactions occur, and a turbo molecular pumped vacuum chamber which houses a quadrupole mass spectrometer and an electron multiplier detector (Mauldin et al., 2003). The measurement technique and system used in this study have been discussed in detail elsewhere (e.g., Tanner et al., 1997; Mauldin et al., 1998, 1999).

The calibration assembly and technique have been described in Mauldin et al. (2001). Briefly, OH was produced by photolyzing a controlled amount of water vapor with a mercury lamp radiation at 184.9 nm. The amount of OH produced depended on water vapor concentration, sample flow



**Fig. 1.** Pictures showing the setup of the LIF and CIMS instruments for OH and HO<sub>2</sub> measurements on the NASA DC-8 aircraft during ARCTAS 2008.

rate, intensity of the mercury lamp, and H<sub>2</sub>O cross section for the 184.9 nm light. During calibrations, flow rates and the ambient dew point were monitored. To determine the photon flux from the lamp at 184.9 nm, vacuum UV photo diodes mounted on an  $x/y$  traverse were used to periodically map out the light field on the ground. The quantum efficiency of these diodes was compared to a National Institute of Standards and Technologies (NIST) standard diode both prior to and after the mission and were found to vary by  $\pm 12\%$ . The CIMS OH instrument was calibrated in flight at different altitudes. Using this calibration method, the overall uncertainty of the OH concentration was  $\pm 65\%$  ( $2\sigma$ ), and the detection limit in a single measurement was  $2 \times 10^5$  molecules cm<sup>-3</sup> (Tanner et al., 1997). For a 5-min integration time, the detection limit for OH was  $5 \times 10^4$  molecules cm<sup>-3</sup> (Mauldin et al., 2001).

### 2.4 CIMS HO<sub>2</sub> instrument

The NCAR PeRCIMS instrument uses a technique based on the amplified chemical conversion of ambient peroxy radicals (HO<sub>2</sub> and/or RO<sub>2</sub>) into a unique ion, HSO<sub>4</sub><sup>-</sup>. Peroxy radicals drawn into the inlet are converted into H<sub>2</sub>SO<sub>4</sub> through the addition of NO and SO<sub>2</sub>. H<sub>2</sub>SO<sub>4</sub> is then reacted with NO<sub>3</sub><sup>-</sup> to form HSO<sub>4</sub><sup>-</sup> ions, which are measured by a quadrupole filter mass spectrometer and a channel electron multiplier. Measurements of the total sum of all peroxy radicals, HO<sub>2</sub> + RO<sub>2</sub> (HO<sub>x</sub>RO<sub>x</sub> mode) or the HO<sub>2</sub> component only (HO<sub>2</sub> mode), can be achieved through adding known concentrations of NO and SO<sub>2</sub> to the sample flow. When inlet [NO] and [SO<sub>2</sub>] are low, RO<sub>2</sub> radicals are converted to HO<sub>2</sub> and can be measured as HO<sub>x</sub>RO<sub>x</sub>. When inlet [NO] and [SO<sub>2</sub>] are high, the conversion efficiency of RO<sub>2</sub> into HO<sub>2</sub> is low and RO<sub>2</sub> radicals are converted to organic nitrates (RONO). A full description of this process and tests of conversion efficiency can be found in Edwards et al. (2003).

Recently, Hornbrook et al. (2011) developed an improved method for PeRCIMS to measure HO<sub>2</sub> and HO<sub>2</sub> + RO<sub>2</sub>. In

this method, both [NO] and [O<sub>2</sub>] are simultaneously varied in the chemical conversion region of the PeRCIMS inlet to change the conversion efficiency of RO<sub>2</sub> to HO<sub>2</sub> so that either primarily HO<sub>2</sub> or HO<sub>2</sub>+ RO<sub>2</sub> are measured. Two modes of operation are established for ambient measurements. In the first half of the minute, RO<sub>2</sub> radicals are measured at close to 100 % efficiency along with HO<sub>2</sub> radicals (low [NO]/[O<sub>2</sub>] =  $2.5 \times 10^{-5}$ ), and in the second half of the minute, HO<sub>2</sub> is detected while the majority of ambient RO<sub>2</sub> radicals are measured with low efficiency, approximately 15 % (high [NO]/[O<sub>2</sub>] =  $6.8 \times 10^{-4}$ ), and the reported HO<sub>2</sub> mixing ratios are corrected for this 15 % RO<sub>2</sub> contribution. This new method was used during ARCTAS.

Calibration of the PeRCIMS instrument was accomplished on the ground only by the photolysis of water vapor using UV radiation (184.9 nm) from a low-pressure mercury lamp (Edwards et al., 2003). Dry synthetic air was first humidified by passing through a saturator containing de-ionized water held at an accurately known temperature (30 °C). The humidified air was diluted with dry synthetic zero air to achieve the desired water/air ratio and the mixture with a total flow rate of about 5 standard liters per minute (SLPM) was passed into a quartz calibration cell. The PeRCIMS sampling flow rate was about 1.9 SLPM. Independent dew point instrumentation measurements of the water mixing ratio indicated that this method can produce accurate H<sub>2</sub>O mixing ratio down to levels approaching 50 ppmv. Water was then photolyzed by the mercury lamp. The radiative output of the mercury lamp used in the calibration was determined through separate N<sub>2</sub>O actinometry experiments (Edwards et al., 2003). Radical mixing ratios over the range of ambient levels and higher/lower values of radicals were easily generated by adjusting the lamp distance, slit width, and water vapor mixing ratio within the photolysis cell. The overall measurement uncertainty associated with this instrument was about  $\pm 50$  % at a  $2\sigma$  confidence level. The detection limit of PeRCIMS during this campaign was about 1.0 pptv ( $2\sigma$ ) with 15-s integration time.

### 2.5 HO<sub>x</sub> measurement comparison strategy

Frequent comparisons between instruments that measure the same atmospheric constituents are essential for producing high-quality data for complex field studies, like ARCTAS, which involve multiple investigators and multiple aircraft. These comparisons often help the investigators produce the highest quality data possible by revealing instrument operation and/or calibration issues, which the investigators can then resolve, sometimes during the field deployment.

During ARCTAS, a comparison strategy was deployed for the measurements of HO<sub>x</sub> as well as many other species measured by different instruments. The field data comparison of these duplicate measurements was “blind”. Within 24 h after each flight, investigators, without knowledge of the other measurements, submitted their data, which was directed to a restricted data depository that was accessible only by a Mea-

surement Comparison Group (MCG). Once all of the duplicate measurements for an atmospheric constituent were in the depository, those measurements were released immediately to the ARCTAS archive. Comparisons of measurements were “blind” only for the field data phase and were not blind for the preliminary and final data submission phases. However, any changes that the investigators made during or after the field campaign had to be accompanied by an explanation of the changes. This explanation had to be submitted to the MCG as well as noted in the data submission header. To aid the post-campaign analysis of the comparisons, all duplicate measurements, from the initial field submission to final data submission, were saved along with the explanations of changes.

### 3 Box model description

The NASA Langley Research Center time-dependent photochemical box model was used to calculate OH, HO<sub>2</sub> and other reactive intermediates. The model has been described in detail in several previous studies (e.g., Crawford et al., 1999; Olson et al., 2006, 2012). The modeling approach was based on the assumption of a diurnal steady state. For a suite of simultaneous measurements of input species at a given point in time, the model integrated to find a self-consistent diurnal cycle for the computed species concentrations based on constraining selected species to the measurements. Computed concentrations at the point in time of measurement were then used as the instantaneous model results. This approach ensured that all computed species were in equilibrium with the diurnal process, which was crucial for species with lifetimes too long for simple instantaneous steady state assumptions. For input, model calculations used observations from the 1-min merged data set available on the ARCTAS public data archive (<ftp://ftp-air.larc.nasa.gov/pub/ARCTAS/>). The minimum set of input constraints included measurements of O<sub>3</sub>, CO, NO, non-methane hydrocarbons (NMHC), H<sub>2</sub>O (dew/frost point), temperature, pressure, and photolysis frequencies. A surface deposition loss of  $1.0 \times 10^{-5} \text{ s}^{-1}$  for modeled species was included in the model for altitudes less than 1 km. Because halogen chemistry is expected to impact surface O<sub>3</sub> chemistry and radical cycling near the surface and in the lower troposphere, the box model was updated to include bromine photochemistry (Olson et al., 2012).

In addition to the required constraints described above, the model had the option to include additional constraints when measurements were available for hydrogen peroxide (H<sub>2</sub>O<sub>2</sub>), methyl hydrogen peroxide (CH<sub>3</sub>OOH), nitric acid (HNO<sub>3</sub>), and peroxy acetyl nitrate (PAN). If unavailable, these atmospheric constituents were calculated by the model based on diurnal steady state. Model calculations taking advantage of these additional constraints were referred to as “constrained”. All model results discussed in this paper were taken from the

standard constrained model simulations in the ARCTAS data archive and may be different from the results presented in Olson et al. (2012), where additional constraints, for example of HCHO, were included.

Sources of uncertainty in model predictions include uncertainties in kinetic and photolytic rate constants, and uncertainties in constraining observations. Estimates of total model uncertainty were obtained using Monte Carlo techniques and a sensitivity approach (Olson et al., 2012).

## 4 Results

### 4.1 Overall intercomparison

Good agreement in general was obtained between the OH and HO<sub>2</sub> measured by CIMS and LIF for the entire three phases of ARCTAS (Fig. 2). The linear regression exhibits  $[\text{OH}]_{\text{CIMS}} = 0.89 \times [\text{OH}]_{\text{LIF}} + 2.8 \times 10^4 \text{ cm}^{-3}$  with a correlation coefficient  $r^2 = 0.72$ , and  $[\text{HO}_2]_{\text{CIMS}} = 0.86 \times [\text{HO}_2]_{\text{LIF}} + 3.9 \text{ pptv}$  with a correlation coefficient  $r^2 = 0.72$ . The dashed lines in Figure 2 represent the combined measurement uncertainties:  $\pm 72\%$  ( $2\sigma$ ) for  $[\text{OH}]_{\text{LIF}}$  and  $[\text{OH}]_{\text{CIMS}}$  and  $\pm 59\%$  ( $2\sigma$ ) for  $[\text{HO}_2]_{\text{LIF}}$  and  $[\text{HO}_2]_{\text{CIMS}}$ . An independent samples t-test (the Student's t-test) was conducted to compare the HO<sub>x</sub> measurements by LIF and by CIMS. Because of their low concentrations during ARCTAS-A, both OH and HO<sub>2</sub> concentrations were averaged into 10-min intervals for this t-test. The t-test results showed that there was no significant difference in the [OH] by LIF (mean =  $(2.6 \pm 2.9) \times 10^6 \text{ cm}^{-3}$ ) and SI-CIMS (mean =  $(2.4 \pm 3.1) \times 10^6 \text{ cm}^{-3}$ ), with a p-value = 0.78. In a Student t-test, a p-value (significance) less than 0.05 is considered to have significant difference. No significant difference was found either in the [HO<sub>2</sub>] by LIF (mean =  $15.1 \pm 12.6 \text{ pptv}$ ) or PeRCIMS (mean =  $17.1 \pm 12.7 \text{ pptv}$ ), with a p-value of 0.76. Both t-tests were conducted at a 95 % confidence level. These results suggest that HO<sub>x</sub> measurements by LIF and CIMS agree generally well and the variation can be largely explained by the relatively large combined measurement uncertainties.

The overall intercomparison of CIMS and LIF HO<sub>x</sub> measurements from each flight is outlined in Table 1. The agreement between CIMS and LIF measurements varies from flight to flight and in the three different phases. For the entire ARCTAS campaign (including ARCTAS-CARB) when both instruments were working, the mean OH concentration was  $2.4 \times 10^6 \text{ cm}^{-3}$  for CIMS and  $2.6 \times 10^6 \text{ cm}^{-3}$  for LIF, with a median CIMS/LIF OH ratio of 0.74. The mean HO<sub>2</sub> mixing ratio was 17.1 pptv for CIMS and 15.1 pptv for LIF, with a median CIMS/LIF OH ratio of 1.29. Among the three phases, the best agreement was obtained during ARCTAS-CARB, with median CIMS/LIF ratios of 0.94 for OH and 1.05 for HO<sub>2</sub>, partially because of relatively high OH and HO<sub>2</sub> mixing ratios during ARCTAS-CARB compared to the

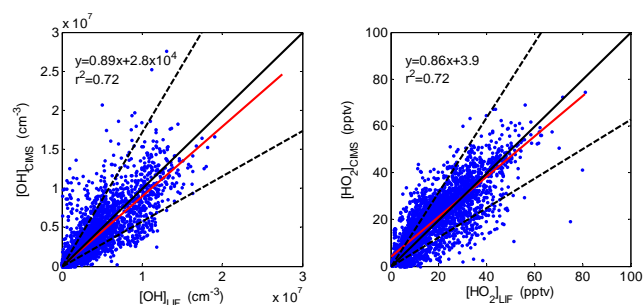


**Fig. 2.** Scatter plots of CIMS [OH] vs. LIF [OH] (left) and CIMS [HO<sub>2</sub>] vs. LIF [HO<sub>2</sub>] (right). The red lines illustrate the linear regression and the black solid lines represent 1 : 1 ratio. The dashed lines indicate the combined measurement uncertainties:  $\pm 72\%$  ( $2\sigma$ ) for OH and  $\pm 59\%$  ( $2\sigma$ ) for HO<sub>2</sub>.

other two phases (Table 1). Relatively larger discrepancies exist during ARCTAS-A, with median CIMS/LIF ratios of 0.72 for OH and 1.65 for HO<sub>2</sub>, mainly due to low levels of OH and HO<sub>2</sub> in the spring in Arctic. During ARCTAS-A, the mean and median OH levels in each flight (except the transit flights from and to Palmdale, California) were below  $1 \times 10^6 \text{ cm}^{-3}$ , and OH concentrations were often lower than or around the detection limits of both instruments. HO<sub>2</sub> mixing ratios were also low during ARCTAS-A, with mean and median levels varying from 2 to 6 pptv if the transit flights from and to Palmdale, California are excluded.

### 4.2 Comparison as a function of altitude

Comparison of OH measurements by CIMS and LIF as a function of altitude shows that at altitudes below 4–5 km, the median CIMS/LIF OH ratios are close to one, but the ratios fall well below 1 above 5 km in all three phases (Fig. 3). These results are very similar to the comparison results from the two previous studies PEM-TB and TRACE-P (Eisele et al., 2001, 2003). During PEM-TB, which was conducted in the tropical Pacific, two brief intercomparisons in close proximity were conducted between the LIF instrument on the NASA DC-8 and the CIMS OH instrument on the NASA P3-B. Excellent agreement was obtained between two aircraft OH measurements in the marine boundary layer, but the CIMS/LIF OH ratio was only about 0.6 at the 5.5-km flight leg. Lower CIMS/LIF OH ratios at higher altitudes were also observed from 25° N latitude to 25° S latitude (Eisele et al., 2001). A similar increasing trend in CIMS/LIF OH ratio at higher altitudes was also observed in three side-by-side flights between the NASA DC-8 and the P-3B during TRACE-P, which was conducted off the coast of Asia with air often quite polluted (Eisele et al., 2003).

The altitude dependence of the CIMS/LIF HO<sub>2</sub> ratio is quite different from that of the OH ratio. During ARCTAS-A, the CIMS HO<sub>2</sub> were consistently higher than the LIF HO<sub>2</sub> by a factor of  $1.72 \pm 0.28$  from the surface to 10 km with little

**Table 1.** Overall comparison of OH and HO<sub>2</sub> measured with LIF and CIMS during ARCTAS.

Flt #	Flight Description	[OH] <sub>CIMS</sub> (cm <sup>-3</sup> )		[OH] <sub>LIF</sub> (cm <sup>-3</sup> )		[OH] <sub>CIMS</sub> /[OH] <sub>LIF</sub>		[HO <sub>2</sub> ] <sub>CIMS</sub> (pptv)		[HO <sub>2</sub> ] <sub>LIF</sub> (pptv)		[HO <sub>2</sub> ] <sub>CIMS</sub> /[HO <sub>2</sub> ] <sub>LIF</sub>	
		mean <sup>a</sup>	median <sup>b</sup>	mean	median	mean	median	mean	median	mean	median	mean	median
1	Palmdale to Fairbanks	–	–	1.4E+06	1.3E+06	–	–	17.0	17.9	10.1	9.4	1.78	1.81
2	Fairbanks to Thule	–	–	4.9E+05	4.7E+05	–	–	4.7	4.5	2.7	2.9	1.82	1.69
3	Thule to Fairbanks	–	–	9.1E+05	8.7E+05	–	–	6.3	5.2	3.3	2.8	1.87	1.88
4	Fairbanks to Iqaluit	1.9E+05	1.6E+05	4.9E+05	4.3E+05	1.29	0.36	3.2	2.9	2.0	2.1	1.81	1.69
5	Iqaluit to Fairbanks	6.5E+05	5.2E+05	6.0E+05	5.1E+05	1.81	1.02	–	–	2.8	2.5	–	–
6	Fairbanks local	4.6E+05	4.6E+05	5.8E+05	5.3E+05	3.78	0.81	–	–	3.2	3.3	–	–
7	Fairbanks local	6.4E+05	6.1E+05	7.2E+05	6.8E+05	1.24	0.85	6.3	5.9	4.3	4.0	1.44	1.45
8	Fairbanks local	3.7E+05	3.0E+05	4.7E+05	4.2E+05	1.46	0.73	4.3	4.3	2.4	2.2	1.84	1.74
9	Fairbanks to Palmdale	1.0E+06	8.0E+05	1.5E+06	1.3E+06	0.72	0.66	12.5	11.9	7.7	7.1	1.67	1.64
	ARCTAS-A (Flt#1-9)	5.2E+05	4.1E+05	6.9E+05	5.6E+05	1.74	0.72	6.3	5.0	3.8	3.0	1.72	1.65
10	Palmdale local	6.5E+06	5.9E+06	8.2E+06	8.1E+06	0.77	0.75	26.7	26.5	28.3	27.9	0.97	0.94
11	Palmdale local	7.1E+06	7.1E+06	7.5E+06	7.5E+06	0.88	0.86	19.6	19.0	28.9	28.5	0.70	0.65
12	Palmdale local	5.3E+06	4.4E+06	4.2E+06	4.1E+06	1.21	1.12	21.0	20.7	17.1	17.2	1.30	1.20
13	Palmdale local	–	–	5.6E+06	4.3E+06	–	–	24.5	21.7	20.0	19.1	1.44	1.25
14	Palmdale to Cold Lake	4.1E+06	3.5E+06	3.9E+06	3.8E+06	1.04	1.02	24.2	25.4	20.3	20.3	1.85	1.14
	ARCTAS-CARB (Flt#10-14)	5.8E+06	4.8E+05	5.9E+06	4.9E+06	1.00	0.92	22.9	21.7	22.5	21.3	1.22	1.05
15	Cold Lake local	2.5E+06	1.6E+06	2.2E+06	2.1E+06	2.15	0.75	15.0	11.5	12.5	9.9	1.45	1.19
16	Cold Lake local	9.7E+06	6.6E+05	1.2E+06	9.4E+05	0.93	0.75	21.6	23.6	14.5	13.7	1.58	1.41
17	Cold Lake local	2.7E+06	1.9E+06	2.3E+06	1.8E+06	1.16	1.07	25.5	27.1	19.7	20.5	1.36	1.28
18	Cold Lake local	2.2E+06	1.1E+06	1.8E+06	1.1E+06	1.27	0.92	14.6	10.7	11.8	8.3	1.06	1.13
19	Cold Lake to Thule	5.6E+05	4.6E+05	9.8E+05	8.4E+05	0.63	0.55	3.4	3.2	2.6	2.2	1.33	1.35
20	Thule local	1.3E+06	1.3E+06	2.3E+06	2.2E+06	0.61	0.58	6.3	4.9	10.8	11.3	0.57	0.46
21	Thule to Cold Lake	1.1E+06	1.0E+06	2.3E+06	2.2E+06	0.51	0.48	13.7	14.0	9.7	9.5	1.49	1.44
22	Cold Lake to Palmdale	2.1E+06	1.5E+06	5.1E+06	3.5E+06	0.41	0.40	38.8	42.7	34.1	35.0	1.23	1.12
	ARCTAS-B (Flt#14-22)	1.7E+06	1.1E+06	1.9E+06	1.7E+06	1.10	0.66	16.4	14.7	12.8	11.0	1.33	1.28
	<b>Entire Campaign</b>	<b>2.4E+06</b>	<b>1.0E+06</b>	<b>2.6E+06</b>	<b>1.6E+06</b>	<b>1.28</b>	<b>0.74</b>	<b>17.1</b>	<b>14.5</b>	<b>15.1</b>	<b>11.4</b>	<b>1.40</b>	<b>1.29</b>

<sup>a</sup> “–” means no CIMS data available for that flight

<sup>b</sup> The mean and median ratios were calculated when both CIMS and LIF measurements were available.

altitude dependence on average (Fig. 4a). This difference is significant considering the combined uncertainty ( $\pm 59\%$ ) of the CIMS and LIF HO<sub>2</sub> measurements. For median ratios in 1-km altitude bins, a Student’s t-test also shows this significant difference between the HO<sub>2</sub> measurements by LIF (mean =  $3.8 \pm 2.6$  pptv) and CIMS (mean =  $6.3 \pm 4.2$  pptv) with a p-value of only 0.02 at a 95 % confidence level. However, during both ARCTAS-CARB and ARCTAS-B, the CIMS/LIF HO<sub>2</sub> ratios are close to 1 below 6 km and Student’s t-tests show no significant difference between the two measurements with p-values of 0.77 for ARCTAS-CARB and 0.15 for ARCTAS-B. Above 6 km, the ratio increases from 1 to 2 (Fig. 4b and c) and the difference is significant.

The reasons for the altitude dependence are unclear. However, as shown in Fig. 5, there is a clear water vapor dependence of the CIMS-to-LIF OH and HO<sub>2</sub> ratios. At lower water mixing ratios ( $< 5000$  ppmv), the CIMS measured OH mixing ratios are smaller than the LIF measured OH on average. When the water mixing ratio is greater than 6000 ppmv, the median CIMS-to-LIF OH ratio is close to 1. The observed CIMS-to-LIF HO<sub>2</sub> ratio exhibits an opposite water vapor dependence compared to the OH ratio. At lower water mixing ratios ( $< 3000$  ppmv), the CIMS measured HO<sub>2</sub> mixing ratios are greater than the LIF measured OH. When the water mixing ratio is greater than 3000 ppmv, the median CIMS-to-LIF HO<sub>2</sub> ratio is close to 1. This water vapor dependence

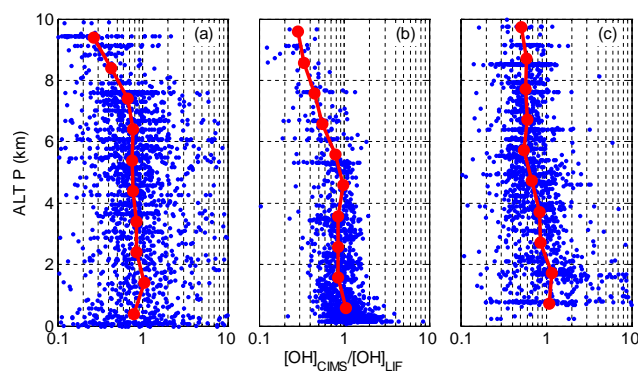


**Fig. 3.** Observed CIMS-to-LIF OH ratio as a function of altitude during ARCTAS-A (a), ARCTAS-CARB (b), and ARCTAS-B (c). Individual points represent 1-min data and linked circles are the median values of 1-km altitude bins.

may be related to the need of water in the CIMS technique to convert OH to H<sub>2</sub>SO<sub>4</sub>.

### 4.3 Comparison with box model

Although this study focuses on the measurement intercomparisons, a comparison with the model results can provide some insight into the measurement differences. In addition, it can indicate potential problems with chemical mechanisms

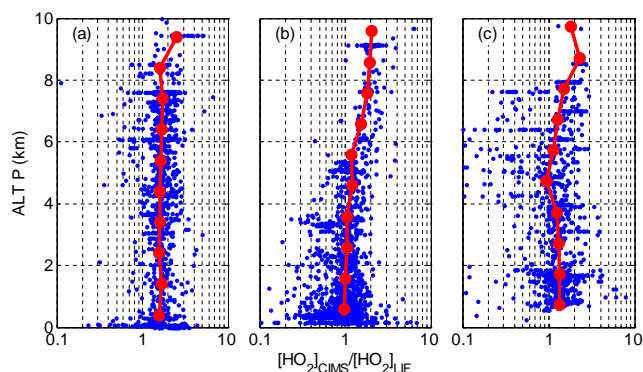


**Fig. 4.** Observed CIMS-to-LIF HO<sub>2</sub> ratio as a function of altitude during ARCTAS-A (a), ARCTAS-CARB (b), and ARCTAS-B (c). Individual points represent 1-min data and linked circles are the median values of 1-km altitude bins.

when measurements from the instruments agree but disagree with the model results. The model simulations with additional constraints including H<sub>2</sub>O<sub>2</sub>, CH<sub>3</sub>OOH, HNO<sub>3</sub>, and PAN were used in this comparison.

In general, the LIF OH agrees well with the modeled OH during ARCTAS-A and ARCTAS-CARB, with little altitude dependence. However, the LIF OH is generally greater than the modeled OH below 8 km during ARCTAS-B, with a median LIF/model OH ratio of 1.3 (Fig. 6). For mean ratios in 1-km altitude bins, Student's t-tests show no significant difference between the measured OH by LIF and the modeled OH with a p-value of 0.42 for ARCTAS-A, 0.66 for ARCTAS-CARB, and 0.47 for ARCTAS-B at a 95 % confidence level.

The CIMS OH agrees well with the modeled OH below 6 km, but falls well below the modeled OH above 6 km during the ARCTAS-A and ARCTAS-CARB phases. During ARCTAS-B, the CIMS OH is in good agreement with the modeled OH between 2–4 km, but the CIMS/model OH ratio is generally greater than 1 below 2 km but less than 1 above 5 km (Fig. 6). Student's t-tests show no significant difference between the CIMS OH and modeled OH for the entire ARCTAS-B (p-value = 0.68) and below 6 km during ARCTAS-A (p-value = 0.52) and ARCTAS-CARB (p-value = 0.91), but show significant difference above 6 km during ARCTAS-A (p-value = 0.006) and ARCTAS-CARB (p-value = 0.001).

For HO<sub>2</sub>, both CIMS and LIF measurements agree with the model below 6 km during ARCTAS-CARB and ARCTAS-B, but the LIF HO<sub>2</sub> is slightly lower and the CIMS HO<sub>2</sub> is slightly greater than the model predictions above 6 km (Fig. 7). During ARCTAS-A, the CIMS HO<sub>2</sub> agrees well with the modeled HO<sub>2</sub> between 2 km and 9 km, although the CIMS HO<sub>2</sub> is slightly greater than the modeled HO<sub>2</sub> for altitudes below 2 km and above 9 km. The median LIF/model HO<sub>2</sub> ratio is 0.79 during ARCTAS-A. For mean ratios in 1-km altitude bins, Student's t-tests show significant difference between the LIF HO<sub>2</sub> and modeled HO<sub>2</sub> during

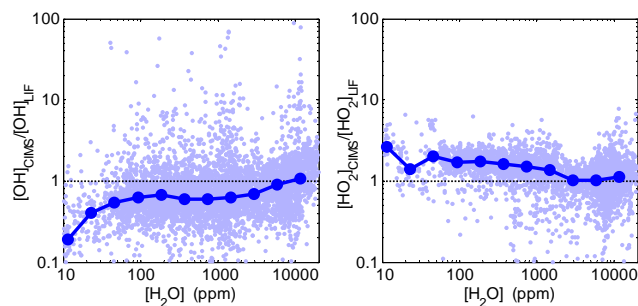


**Fig. 5.** Observed CIMS-to-LIF ratios of OH (left) and HO<sub>2</sub> (right) as a function of water mixing ratio. Individual points represent 1-minute data for the entire ARCTAS mission and linked circles are the median values of water mixing ratio bins. The dotted lines indicate a ratio of 1.

ARCTAS-A (p-value = 0.008), but no significant difference during ARCTAS-CARB (p-value = 0.72) and ARCTAS-B (p-value = 0.07). The t-tests also show significant difference between the CIMS HO<sub>2</sub> and modeled HO<sub>2</sub> during ARCTAS-CARB (p-value = 0.04), but no significant difference during ARCTAS-A (p-value = 0.68) and ARCTAS-B (p-value = 0.48). In fact, an HO<sub>2</sub> uptake by aerosols has been proposed to explain this model overestimate of LIF HO<sub>2</sub> during ARCTAS-A (Mao et al., 2010). However, a recent study by Olson et al. (2012) shows that the parameterization suggested by Mao et al. (2010) is insufficient to reconcile the discrepancy between model and LIF observations. We attribute this in part to the large uncertainties associated with the measurements of HO<sub>x</sub> precursors (Olson et al., 2012) and aerosol surface area (particularly hygroscopicity), and in part to an underestimate of HO<sub>2</sub> uptake coefficient (J. Mao, S. Fan and D. J. Jacob, Radical loss in the atmosphere from Cu–Fe redox coupling in aerosols, submitted). This HO<sub>2</sub> uptake was expected to have less impact on HO<sub>2</sub> concentrations during ARCTAS-CARB and ARCTAS-B because of the relatively fast gas-phase photochemistry during these two phases.

#### 4.4 Comparison as a function of NO

Nitric oxide (NO) plays a key role in HO<sub>x</sub> photochemistry by cycling HO<sub>2</sub> to OH, so it is important to conduct observation-to-model comparisons as a function of NO. The observed-to-modeled HO<sub>2</sub> ratio increases for higher NO levels, as seen by both LIF and CIMS (Fig. 8, middle). This hints that there are missing HO<sub>x</sub> sources in the model that correlate with NO. When the model was constrained to the measured H<sub>2</sub>O<sub>2</sub> and HCHO, the measured-to-modeled HO<sub>2</sub> ratio is 0.69 for NO < 100 pptv and 1.2 for NO > 100 pptv. The trend of the higher-than-predicted HO<sub>2</sub> at high NO remains with these additional constraints (Olson et al., 2012). The modeled OH is lower than the LIF OH at low NO levels but lower than the CIMS OH at high NO levels, indicating that there is difference between LIF and CIMS measurements

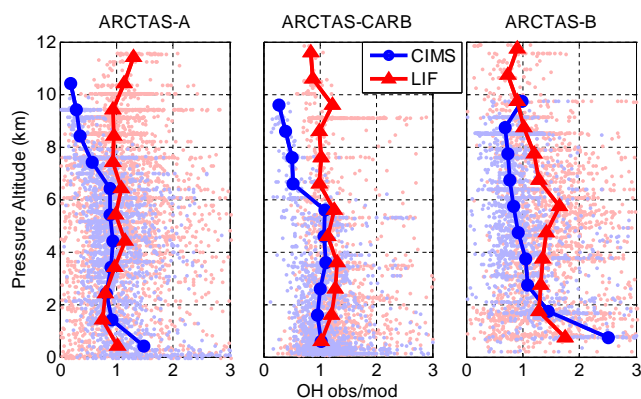


**Fig. 6.** Measured-to-modeled OH as a function of altitude during ARCTAS-A (left), ARCTAS-CARB (middle) and ARCTAS-B (right) phases of ARCTAS. Comparisons of the box model with CIMS (blue) and LIF (red) are shown as 1-min measurements (small dots) and as 1-km median values (linked symbols).

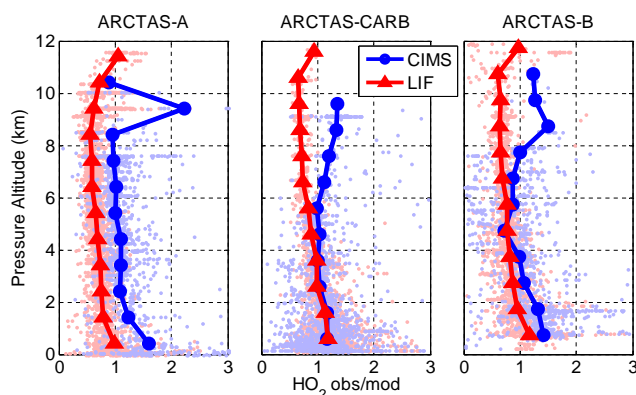


**Fig. 7.** Measured-to-modeled HO<sub>2</sub> as a function of altitude during ARCTAS-A (left), ARCTAS-CARB (middle) and ARCTAS-B (right). Comparisons of the box model with CIMS (blue) and LIF (red) are shown as 1-minute measurements (small dots) and as median values in 1-km bins (linked symbols).

at low and high NO mixing ratios. When the NO levels are between  $\sim 10$  pptv and  $\sim 1$  parts per billion by volume (ppbv, equivalent to  $\text{nmol mol}^{-1}$ ), the observed-to-modeled OH ratios are close to 1 for both LIF and CIMS. Because of the higher CIMS OH than the modeled OH at high NO levels, the observed-to-modeled HO<sub>2</sub>/OH ratios for CIMS are close to 1 despite the higher-than-expected HO<sub>2</sub> at high NO levels (Fig. 8, bottom). For LIF, the observed-to-modeled HO<sub>2</sub>/OH ratio increases as NO level increases, consistent with the gradual increasing of the observed-to-modeled HO<sub>2</sub> ratio as NO increases. Interpretation of these trends at higher NO must be tempered by the fact that during ARCTAS 90 % of the NO mixing ratios were less than 100 pptv, so there are limited data points at higher NO (e.g., NO > 1 ppbv).

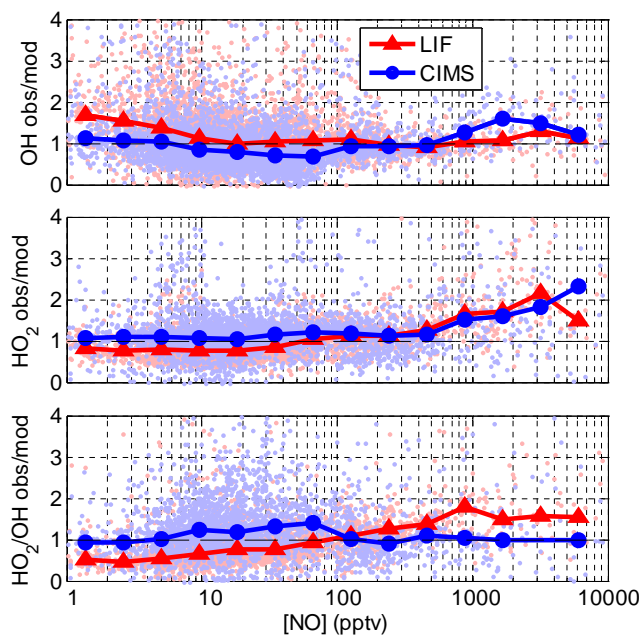


**Fig. 8.** NO dependence of observed-to-modeled OH (top) and HO<sub>2</sub> (middle) and HO<sub>2</sub>/OH (bottom) ratios for LIF (red) and CIMS (blue) measurements during ARCTAS. Individual points are 1-min averaged data and linked symbols indicate median values in NO mixing ratio bins.

For the median values, Student's t-tests show no significant difference either between the CIMS OH and LIF OH ( $p$ -value = 0.91) or between the CIMS HO<sub>2</sub> and LIF HO<sub>2</sub> ( $p$ -value = 0.78) as a function of NO for the entire ARCTAS.

#### 4.5 Comparison as a function of isoprene

Similar to the Intercontinental Chemical Transport Experiment-A (INTEX-A) in 2004 and the Program for Research on Oxidants: Photochemistry, Emissions and Transport in summer 1998 (PROPHET 1998) (Ren et al., 2008), the observed-to-modeled OH ratio is frequently much greater than 1.0 below 2-km altitude at high isoprene levels during ARCTAS-CARB and ARCTAS-B (Fig. 9). More interestingly, very similar isoprene dependence of observed-to-modeled OH ratio was observed for both CIMS and LIF, two fundamentally different techniques. The observed-to-modeled OH ratio increases slowly from 1.0 to 2 as isoprene increases from less than 20 pptv to 500 pptv, but for isoprene levels exceeding 500 pptv, the observed-to-modeled OH ratio rapidly increases to  $\sim 6$  as isoprene increases to 6–8 ppbv. In contrast, the observed-to-modeled HO<sub>2</sub> ratios have little dependence on isoprene for both CIMS and LIF (Fig. 9). For the median values, Student's t-tests show no significant difference either between the CIMS OH and LIF OH ( $p$ -value = 0.88), or between the CIMS HO<sub>2</sub> and LIF

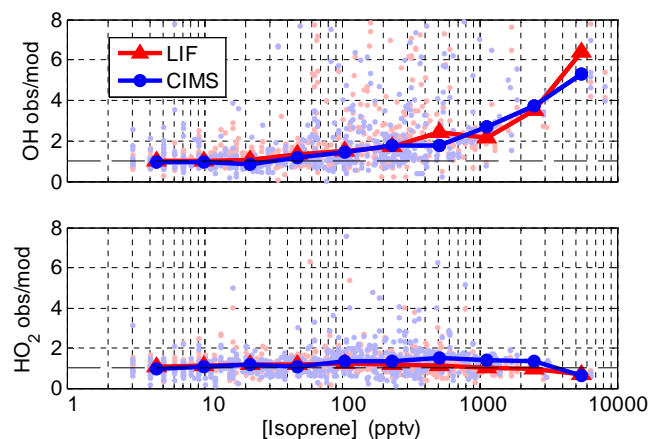


**Fig. 9.** Observed-to-modeled OH (top) and HO<sub>2</sub> (bottom) ratios for LIF (red) and CIMS (blue) measurements as a function of isoprene. Individual points are 1-min averaged data and linked symbols indicate median values in isoprene mixing ratio bins.

HO<sub>2</sub> (p-value = 0.32) as a function of isoprene for the entire ARCTAS.

The reasons for the higher-than-expected measured OH at high isoprene levels are not clear, but much of the discrepancy for the ATHOS LIF OH can be explained by an unknown measured interference. The OH concentrations measured by LIF are likely higher than the actual values in environments when biogenic emissions dominate (Mao et al., 2012). A new chemical removal method using hexafluoropropylene (C<sub>3</sub>F<sub>6</sub>) to measure OH was deployed in parallel with the traditional FAGE method during BEARPEX 2009, a field intensive study in a California forest east of Sacramento. The new method gives on average only 40–50 % of the OH from the traditional method. The discrepancy was found to be temperature-dependent, with less influence under lower temperatures. The interference is possibly due to internally generated OH, likely from oxidation of biogenic volatile organic compounds. Unfortunately, this new chemical removal method was not used for the LIF OH measurements during ARCTAS, so the level of this interference could not be quantified. It is unclear why the measured-to-modeled OH ratios for CIMS and LIF agree so well as a function of isoprene during ARCTAS, although there are few published papers on intercomparisons between LIF and CIMS OH measurements in forests. One such comparison is HO<sub>x</sub>COMP. While the OH measured by CIMS was found to be less than the OH measured by LIF during HO<sub>x</sub>Comp, the difference have been attributed to sampling inhomogeneities and calibration problems (Schlosser et al., 2009). In a boreal forest in Hyytiälä, southern Finland, CIMS OH measurements were surprisingly lower than modeled values and missing VOCs in the model might act as an OH sink (Petäjä et al., 2009). In a more recent LIF–DOAS OH intercomparison study in chamber experiments with high VOC but low NO<sub>x</sub> levels,

the scatter plot of LIF and DOAS had a slope of 1.02 and an intercept of  $1.0 \times 10^5 \text{ cm}^{-3}$ , indicating general agreement between the two techniques. However, LIF measurements were about 30–40 % larger than those by DOAS after methylvinyl ketone (MVK) and toluene had been added (Fuchs et al., 2012), indicating a possible interference that the authors said they would investigate in the laboratory. Apparently both LIF and CIMS instruments need to be further tested in the laboratory regarding potential instrument artifacts in environments where biogenic emissions dominate.

At the same time, the amount of OH production from isoprene oxidation is still being debated. A few recent studies have suggested regeneration of OH in the photooxidation of isoprene either through the formation of epoxides (Paulot et al., 2009) or isomerization of isoprene peroxy radicals (Peeters et al., 2009; Peeters and Müller, 2010). These mechanisms of OH regeneration in isoprene oxidation have not been included in the current box model simulations for ARCTAS. Including these mechanisms in the model might shed light on some of the discrepancy.

## 5 Summary

A formal intercomparison of OH and HO<sub>2</sub> measured with two fundamentally different techniques, LIF and CIMS, was conducted successfully for the first time on the same aircraft platform during ARCTAS. Good agreement in general was observed. Linear regression results show that  $[\text{OH}]_{\text{CIMS}} = 0.89 \times [\text{OH}]_{\text{LIF}} + 2.8 \times 10^4 \text{ cm}^{-3}$  with a correlation coefficient  $r^2 = 0.72$  for OH, and  $[\text{HO}_2]_{\text{CIMS}} = 0.86 \times [\text{HO}_2]_{\text{LIF}} + 3.9 \text{ pptv}$  with a correlation coefficient  $r^2 = 0.72$  for HO<sub>2</sub>. The difference between the CIMS and LIF instruments for OH and HO<sub>2</sub> measurements can be generally explained by their combined measurement uncertainties.

Comparison with box model results shows some similarities for both CIMS and LIF measurements. First, the observed-to-modeled HO<sub>2</sub> ratio increases greatly for higher NO levels, indicating that the model may miss HO<sub>x</sub> sources that correlate with elevated NO. Second, the observed-to-modeled OH ratio in the planetary boundary layer in forested regions is a strong function of isoprene. It increases slowly from 1.0 to 2.0 as isoprene increases from ~20 pptv to 500 pptv, but for isoprene levels exceeding 500 pptv, the observed-to-modeled OH ratio rapidly increased to ~6. This isoprene dependence of observed-to-modeled OH ratio is consistent with the results in INTEX-A and PROPHET 1998, indicating either incomplete understanding of isoprene chemistry in the model or an interference in the measurements in environments where biogenic emissions dominate ambient volatile organic compounds.

**Supplementary material related to this article is available online at:** <http://www.atmos-meas-tech.net/5/2025/2012/amt-5-2025-2012-supplement.pdf>.

*Acknowledgements.* This work was supported by the NASA Tropospheric Chemistry Program (NNH07ZDA001N-ARCTAS and NNX08AH67G). The authors thank the DC-8 management, crew, and support staff during the ARCTAS preparation and deployment, other ARCTAS research groups for the use of their data in the model, and D. M. Shelow, A. Ortega, and L. Zhang for help in the field and laboratory experiments. The authors also thank the editor and the two anonymous reviewers for providing valuable comments.

Edited by: J. Stutz

## References

- Armerding, W., Spiekermann, M., and Comes, F. J.: OH multipass absorption: Absolute and in situ method for local monitoring of tropospheric hydroxyl radicals, *J. Geophys. Res.*, 99, 1225–1239, 1994.
- Berresheim, H., Elste, T., Plass-Dülmer, C., Eisele, F. L., and Tanner, D. J.: Chemical ionization mass spectrometer for long-term measurements of atmospheric OH and H<sub>2</sub>SO<sub>4</sub>, *Int. J. Mass Spectrom.*, 202, 91–109, 2000.
- Brauers, T., Aschmutat, U., Brandenburger, U., Dorn, H.-P., Hausmann, M., Heßling, M., Hofzumahaus, A., Holland, F., Plass-Dulmer, C., and Ehhalt, D. H.: Intercomparison of tropospheric OH radical measurements by multiple folded long-path laser absorption and laser induced fluorescence, *Geophys. Res. Lett.*, 23, 2545–2548, 1996.
- Brune, W. H., Stevens, P. S., and Mather, J. H.: Measuring OH and HO<sub>2</sub> in the troposphere by laser-induced fluorescence at low pressure, *J. Atmos. Sci.*, 52, 3328–3336, 1995.
- Campbell, M. J., Hall, B. D., Sheppard, J. C., Utley, P. L., O'Brien, R. J., Hard, T. M., and George, L. A.: Intercomparison of local hydroxyl measurements by radiocarbon and FAGE techniques, *J. Atmos. Sci.*, 52, 3421–3427, 1995.
- Commane, R., Floquet, C. F. A., Ingham, T., Stone, D., Evans, M. J., and Heard, D. E.: Observations of OH and HO<sub>2</sub> radicals over West Africa, *Atmos. Chem. Phys.*, 10, 8783–8801, doi:10.5194/acp-10-8783-2010, 2010.
- Crawford, J., Davis, D., Olson, J., Chen, G., Liu, S., Gregory, G., Barrick, J., Sachse, G., Sandholm, S., Heikes, B., Singh, H., and Blake, D.: Assessment of upper tropospheric HO<sub>x</sub> source over the tropical Pacific based on NASA GTE/PEM data: Net affect on HO<sub>x</sub> and other photochemical parameters, *J. Geophys. Res.*, 104, 16255–16273, 1999.
- Di Carlo, P., Brune, W. H., Martinez, M., Harder, H., Leshner, R., Ren, X., Thornberry, T., Carroll, M. A., Young, V., Shepson, P. B., Riemer, D., Apel, E., and Campbell, C.: Missing OH reactivity in a forest: Evidence for unknown reactive biogenic VOCs, *Science* 304, 722–725, 2004.
- Dusanter, S., Vimal, D., and Stevens, P. S.: Technical note: Measuring tropospheric OH and HO<sub>2</sub> by laser-induced fluorescence at low pressure. A comparison of calibration techniques, *Atmos. Chem. Phys.*, 8, 321–340, doi:10.5194/acp-8-321-2008, 2008.
- Edwards, G. D., Cantrell, C. A., Stephens, S., Hill, B., Goyea, O., Shetter, R. E., Mauldin, R. L., Kosciuch, E., Tanner D. J., and Eisele, F. L.: Chemical Ionization Mass Spectrometer instrument for the measurement of tropospheric HO<sub>2</sub> and RO<sub>2</sub>, *Anal. Chem.*, 75, 5317–5327, 2003.
- Ehhalt, D. H., Dorn, H.-P., and Poppe, D.: The chemistry of the hydroxyl radical in troposphere, *Proc. Royal. Soc. Ed.* 97B, 17–34, 1991.
- Eisele, F. L. and Tanner, D. J.: Ion-assisted tropospheric OH measurements, *J. Geophys. Res.*, 96, 9295–9308, 1991.
- Eisele, F. L., Mount, G. H., Fehsenfeld, F. C., Harder, J., Marovich, E., Parrish, D. D., Roberts, J., Trainer, M., and Tanner, D.: Intercomparison of tropospheric OH and ancillary trace gas measurements at Fritz Peak Observatory, Colorado, *J. Geophys. Res.*, 99, 18605–18626, 1994.
- Eisele, F. L., Mauldin, R. L., Ranner, D. J., Cantrell, C., Kosciuch, E., Nowak, J. B., Brune, B., Faloon, I., Tan, D., Davis, D. D., Wang, L., and Chen, G.: Relationship between OH measurements on two different NASA aircraft during PEM Tropics B, *J. Geophys. Res.*, 106, 32683–32689, 2001.
- Eisele, F. L., Mauldin, L., Cantrell, C., Zondlo, M., Apel, E., Fried, A., Walega, J., Shetter, R., Lefer, B., Flocke, F., Weinheimer, A., Avery, M., Vay, S., Sachse, G., Podolske, J., Diskin, G., Barrick, J. D., Singh, H. B., Brune, W., Harder, H., Martinez, M., Bandy, A., Thornton, D., Heikes, B., Kondo, Y., Riemer, D., Sandholm, S., Tan, D., Talbot, R., and Dibb, J.: Summary of measurement intercomparisons during TRACE-P, *J. Geophys. Res.*, 108, 8791, doi:10.1029/2002JD003167, 2003.
- Faloon, I., Tan, D., Brune, W., Hurst, J., Barkat Jr., D., Couch, T. L., Shepson, P., Apel, E., Riemer, D., Thornberry, T., Carroll, M. A., Sillman, S., Keeler, G. J., Sagady, J., Hooper, D., and Paterson, K.: Nighttime observations of anomalously high levels of hydroxyl radicals above a deciduous forest canopy, *J. Geophys. Res.*, 106, 24315–24333, 2001.
- Faloon, I. C., Tan, D., Leshner, R. L., Hazen, N. L., Frame, C. L., Simpas, J. B., Harder, H., Martinez, M., Di Carlo, P., Ren, X., and Brune, W. H.: A laser-induced fluorescence instrument for detecting tropospheric OH and HO<sub>2</sub>: Characteristics and calibration, *J. Atmos. Chem.*, 47, 139–167, 2004.
- Fuchs, H., Brauers, T., Häseler, R., Holland, F., Mihelcic, D., Müsgen, P., Rohrer, F., Wegener, R., and Hofzumahaus, A.: Intercomparison of peroxy radical measurements obtained at atmospheric conditions by laser-induced fluorescence and electron spin resonance spectroscopy, *Atmos. Meas. Tech.*, 2, 55–64, doi:10.5194/amt-2-55-2009, 2009.
- Fuchs, H., Brauers, T., Dorn, H.-P., Harder, H., Häseler, R., Hofzumahaus, A., Holland, F., Kanaya, Y., Kajii, Y., Kubistin, D., Lou, S., Martinez, M., Miyamoto, K., Nishida, S., Rudolf, M., Schlosser, E., Wahner, A., Yoshino, A., and Schurath, U.: Technical Note: Formal blind intercomparison of HO<sub>2</sub> measurements in the atmosphere simulation chamber SAPHIR during the HO<sub>x</sub>Comp campaign, *Atmos. Chem. Phys.*, 10, 12233–12250, doi:10.5194/acp-10-12233-2010, 2010.
- Fuchs, H., Bohn, B., Hofzumahaus, A., Holland, F., Lu, K. D., Nehr, S., Rohrer, F., and Wahner, A.: Detection of HO<sub>2</sub> by laser-induced fluorescence: calibration and interferences from RO<sub>2</sub> radicals, *Atmos. Meas. Tech.*, 4, 1209–1225, doi:10.5194/amt-4-1209-2011, 2011.
- Fuchs, H., Dorn, H.-P., Bachner, M., Bohn, B., Brauers, T., Gomm, S., Hofzumahaus, A., Holland, F., Nehr, S., Rohrer, F., Tillmann, R., and Wahner, A.: Comparison of OH concentration measurements by DOAS and LIF during SAPHIR chamber experiments at high OH reactivity and low NO concentration, *Atmos. Meas. Tech.*, 5, 1611–1626, doi:10.5194/amt-5-1611-2012, 2012.

- Hanke, M., Uecker, J., Reiner, T., and Arnold, F.: Atmospheric peroxy radicals: ROXMAS, a new mass-spectrometric methodology for speciated measurements of HO<sub>2</sub> and RO<sub>2</sub> and first results, *Int. J. Mass Spectrom.*, 213, 91–99, 2002.
- Hard, T. M., O'Brian, R. J., Chan, C. Y., and Mehrabzadeh, A. A.: Tropospheric free radical determination by FAGE, *Environ. Sci. Technol.*, 18, 768–777, 1984.
- Heal, M. R., Heard, D. E., Pilling, M. J., and Whitker, B. J.: On the development and validation of FAGE for local measurement of tropospheric OH and HO<sub>2</sub>, *J. Atmos. Sci.*, 52, 3428–3441, 1995.
- Hofzumahaus, A., Aschmutat, U., Brandenburger, U., Brauers, T., Dorn, H.-P., Hausmann, M., Hessling, M., Holland, F., and Plass-Dülmer, C.: Intercomparison of tropospheric OH measurements by different laser techniques during the POPCORN campaign 1994, *J. Atmos. Chem.*, 31, 227–246, 1998.
- Hofzumahaus, A., Rohrer, F., Lu, K., Bohn, B., Brauers, T., Chang, C.-C., Fuchs, H., Holland, F., Kita, K., Kondo, Y., Li, X., Lou, S., Shao, M., Zeng, L., Wahner, A., and Zhang, Y.: Amplified trace gas removal in the troposphere, *Science*, 324, 1702–1704, doi:10.1126/science.1164566, 2009.
- Holland, F., Hessling, M., and Hofzumahaus, A.: In situ measurement of tropospheric OH radicals by laser-induced fluorescence – a description of the KFA instrument, *J. Atmos. Sci.*, 52, 3393–3401, 1995.
- Hornbrook, R. S., Crawford, J. H., Edwards, G. D., Goyea, O., Mauldin III, R. L., Olson, J. S., and Cantrell, C. A.: Measurements of tropospheric HO<sub>2</sub> and RO<sub>2</sub> by oxygen dilution modulation and chemical ionization mass spectrometry, *Atmos. Meas. Tech.*, 4, 735–756, doi:10.5194/amt-4-735-2011, 2011.
- Jacob, D. J., Crawford, J. H., Maring, H., Clarke, A. D., Dibb, J. E., Emmons, L. K., Ferrare, R. A., Hostetler, C. A., Russell, P. B., Singh, H. B., Thompson, A. M., Shaw, G. E., McCauley, E., Pederson, J. R., and Fisher, J. A.: The Arctic Research of the Composition of the Troposphere from Aircraft and Satellites (ARCTAS) mission: design, execution, and first results, *Atmos. Chem. Phys.*, 10, 5191–5212, doi:10.5194/acp-10-5191-2010, 2010.
- Kanaya, Y., Sadanaga, Y., Hirokawa, Kajii, Y., and Akimoto, H.: Development of a ground-based LIF instrument for measuring HO<sub>x</sub> radicals: Instrumentation and calibrations, *J. Atmos. Chem.*, 38, 73–110, 2001.
- Kanaya, Y., Hofzumahaus, A., Dorn, H.-P., Brauers, T., Fuchs, H., Holland, F., Rohrer, F., Bohn, B., Tillmann, R., Wegener, R., Wahner, A., Kajii, Y., Miyamoto, K., Nishida, S., Watanabe, K., Yoshino, A., Kubistin, D., Martinez, M., Rudolf, M., Harder, H., Berresheim, H., Elste, T., Plass-Dülmer, C., Stange, G., Kliffmann, J., Elshorbany, Y., and Schurath, U.: Comparisons of observed and modeled OH and HO<sub>2</sub> concentrations during the ambient measurement period of the HO<sub>x</sub>Comp field campaign, *Atmos. Chem. Phys.*, 12, 2567–2585, doi:10.5194/acp-12-2567-2012, 2012.
- Kleb, M. M., Chen, G., Crawford, J. H., Flocke, F. M., and Brown, C. C.: An overview of measurement comparisons from the INTEX-B/MILAGRO airborne field campaign, *Atmos. Meas. Tech.*, 4, 9–27, doi:10.5194/amt-4-9-2011, 2011.
- Lelieveld, J., Dentener, F. J., Peters, W., and Krol, M. C.: On the role of hydroxyl radicals in the self-cleansing capacity of the troposphere, *Atmos. Chem. Phys.*, 4, 2337–2344, doi:10.5194/acp-4-2337-2004, 2004.
- Lelieveld, J., Butler, T. M., Crowley, J., Dillon, T., Fischer, H., Ganzeveld, L., Harder, H., Lawrence, M. G., Martinez, M., Taraborrelli, D., and Williams, J.: Atmospheric oxidation capacity sustained by a tropical forest, *Nature*, 452, 737–740, 2008.
- Logan, J. A., Prather, M. J., Wofsy, S. C., and McElroy, M. B.: Tropospheric chemistry: A global perspective, *J. Geophys. Res.*, 86, 7210–7254, 1981.
- Lu, K. D., Rohrer, F., Holland, F., Fuchs, H., Bohn, B., Brauers, T., Chang, C. C., Häseler, R., Hu, M., Kita, K., Kondo, Y., Li, X., Lou, S. R., Nehr, S., Shao, M., Zeng, L. M., Wahner, A., Zhang, Y. H., and Hofzumahaus, A.: Observation and modelling of OH and HO<sub>2</sub> concentrations in the Pearl River Delta 2006: a missing OH source in a VOC rich atmosphere, *Atmos. Chem. Phys.*, 12, 1541–1569, doi:10.5194/acp-12-1541-2012, 2012.
- Mao, J., Jacob, D. J., Evans, M. J., Olson, J. R., Ren, X., Brune, W. H., Clair, J. M. St., Crounse, J. D., Spencer, K. M., Beaver, M. R., Wennberg, P. O., Cubison, M. J., Jimenez, J. L., Fried, A., Weibring, P., Walega, J. G., Hall, S. R., Weinheimer, A. J., Cohen, R. C., Chen, G., Crawford, J. H., McNaughton, C., Clarke, A. D., Jaeglé, L., Fisher, J. A., Yantosca, R. M., Le Sager, P., and Carouge, C.: Chemistry of hydrogen oxide radicals (HO<sub>x</sub>) in the Arctic troposphere in spring, *Atmos. Chem. Phys.*, 10, 5823–5838, doi:10.5194/acp-10-5823-2010, 2010.
- Mao, J., Ren, X., Brune, W. H., Van Duin, D. M., Cohen, R. C., Park, J.-H., Goldstein, A. H., Paulot, F., Beaver, M. R., Crounse, J. D., Wennberg, P. O., DiGangi, J. P., Henry, S. B., Keutsch, F. N., Park, C., Schade, G. W., Wolfe, G. M., and Thornton, J. A.: Insights into hydroxyl measurements and atmospheric oxidation in a California forest, *Atmos. Chem. Phys. Discuss.*, 12, 6715–6744, doi:10.5194/acpd-12-6715-2012, 2012.
- Mao, J., Ren, X., Chen, S., Brune, W. H., Chen, Z., Martinez, M., Harder, H., Lefer, B., Rappenglück, B., Flynn, J., and Leuchner, M.: Atmospheric oxidation capacity in the summer of Houston 2006: Comparison with summer measurements in other metropolitan studies, *Atmos. Environ.*, 44, 4107–4115, 2010.
- Martinez, M., Harder, H., Kubistin, D., Rudolf, M., Bozem, H., Eerdeken, G., Fischer, H., Klüpfel, T., Gurk, C., Königstedt, R., Parchatka, U., Schiller, C. L., Stickler, A., Williams, J., and Lelieveld, J.: Hydroxyl radicals in the tropical troposphere over the Suriname rainforest: airborne measurements, *Atmos. Chem. Phys.*, 10, 3759–3773, doi:10.5194/acp-10-3759-2010, 2010.
- Mather, J. H., Stevens, P. S., and Brune, W. H.: OH and HO<sub>2</sub> measurements using laser-induced fluorescence, *J. Geophys. Res.*, 102, 6427–6436, 1997.
- Mauldin III, R. L., Tanner, D. J., Frost, G. J., Chen, G., Prevot, A. S. H., Davis, D. D., and Eisele, F. L.: OH measurements during ACE-1: observations and model comparisons, *J. Geophys. Res.*, 103, 16713–16729, 1998.
- Mauldin III, R. L., Tanner, D. J., Frost, G. J., Chen, G., Prevot, A. S. H., Davis, D. D., and Eisele, F. L.: OH measurements during PEM-Tropics A, *J. Geophys. Res.* 104, 5817–5827, 1999.
- Mauldin, R. L., III, Eisele, F. L., Cantrell, C. A., Kosciuch, E., Ridley, B. A., Lefer, B., Tanner, D. J., Nowak, J. B., Chen, G., Wang, L., and Davis, D.: Measurements of OH aboard the NASA P-3 during PEM-Tropics B, *J. Geophys. Res.*, 106, 32657–32666, 2001.
- Mauldin III, R. L., Cantrell, C. A., Zondlo, M., Kosciuch, E., Eisele, F. L., Chen, G., Davis, D., Weber, R., Crawford, J., Blake, D., Bandy, A., and Thornton, D.: Highlights of OH, H<sub>2</sub>SO<sub>4</sub>, and

- methane sulfonic acid measurements made aboard the NASA P-3B during Transport and Chemical Evolution over the Pacific, *J. Geophys. Res.*, 108, 8796, doi:10.1029/2003JD003410, 2003.
- Mount, G. H., Eisele, F. L., Tanner, D. J., Brault, J. W., Johnston, P. V., Harder, J. W., Williams, E. J., Fried, A., and Shetter, R.: An intercomparison of spectroscopic laser long-path and ion-assisted in situ measurements of hydroxyl concentrations during the Tropospheric OH Photochemistry Experiment, fall 1993, *J. Geophys. Res.*, 102, 6437–6455, 1997.
- Olson, J. R., Crawford, J. H., Chen, G., Brune, W. H., Faloona, I. C., Tan, D., Harder, H., and Martinez, M.: A reevaluation of airborne HO<sub>x</sub> observations from NASA field campaigns, *J. Geophys. Res.*, 111, D10301, doi:10.1029/2005JD006617, 2006.
- Olson, J. R., Crawford, J. H., Brune, W., Mao, J., Ren, X., Fried, A., Anderson, B., Apel, E., Beaver, M., Blake, D., Chen, G., Crounse, J., Dibb, J., Diskin, G., Hall, S. R., Huey, L. G., Knapp, D., Richter, D., Riemer, D., Clair, J. St., Ullmann, K., Walega, J., Weibring, P., Weinheimer, A., Wennberg, P., and Wisthaler, A.: An analysis of fast photochemistry over high northern latitudes during spring and summer using in-situ observations from ARCTAS and TOPSE, *Atmos. Chem. Phys.*, 12, 6799–6825, doi:10.5194/acp-12-6799-2012, 2012.
- Paulot, F., Crounse, J. D., Kjaergaard, H. G., Kürten, A., St. Clair, J. M., Seinfeld, J. H., and Wennberg, P. O.: Unexpected epoxide formation in the gas-phase photooxidation of isoprene, *Science*, 325, 730–733, doi:10.1126/science.1172910, 2009.
- Peeters, J. and Müller, J.-F.: HO<sub>x</sub> radical regeneration in isoprene oxidation via peroxy radical isomerisations, II: Experimental evidence and global impact, *Phys. Chem. Chem. Phys.*, 12, 14227–14235, 2010.
- Peeters, J., Nguyen, T. L., and Vereecken, L.: HO<sub>x</sub> radical regeneration in the oxidation of isoprene, *Phys. Chem. Chem. Phys.*, 11, 5935–5939, 2009.
- Perner, D., Ehhalt, D. H., Pätz, H.-W., Platt, U., Röth, E. P., and Volz, A.: OH radicals in the lower troposphere, *Geophys. Res. Lett.*, 3, 466–468, 1976.
- Petäjä, T., Mauldin, III, R. L., Kosciuch, E., McGrath, J., Nieminen, T., Paasonen, P., Boy, M., Adamov, A., Kotiaho, T., and Kulmala, M.: Sulfuric acid and OH concentrations in a boreal forest site, *Atmos. Chem. Phys.*, 9, 7435–7448, doi:10.5194/acp-9-7435-2009, 2009.
- Ren, X., Edwards, G. D., Cantrell, C. A., Leshner, R. L., Metcalf, A. R., Shirley, T., and Brune, W. H.: Intercomparison of peroxy radical measurements at a rural site using laser-induced fluorescence and Peroxy Radical Chemical Ionization Mass Spectrometer (PeRCIMS) techniques, *J. Geophys. Res.*, 108, 4605, doi:10.1029/2003JD003644, 2003.
- Ren, X., Brune, W. H., Cantrell, C. A., Edwards, G. D., Shirley, T., Metcalf, A. R., and Leshner, R. L.: Hydroxyl and peroxy radical chemistry in a rural area of Central Pennsylvania: Observations and model comparisons, *J. Atmos. Chem.*, 52, 231–257, 2005.
- Ren, X., Olson, J. R., Crawford, J. H., Brune, W. H., Mao, J., Long, R. B., Chen, Z., Chen, G., Avery, M. A., Sachse, G. W., Barrick, J. D., Diskin, G. S., Huey, L. G., Fried, A., Cohen, R. C., Heikes, B., Wennberg, P. O., Singh, H. B., Blake, D. R., and Shetter, R. E.: HO<sub>x</sub> chemistry during INTEX-A 2004: Observation, model calculation, and comparison with previous studies, *J. Geophys. Res.*, 113, D05310, doi:10.1029/2007JD009166, 2008.
- Schlosser, E., Bohn, B., Brauers, T., Dorn, H.-P., Fuchs, H., Häsel, R., Hofzumahaus, A., Holland, F., Rohrer, F., Rupp, L. O., Siese, M., Tillmann, R., and Wahner, A.: Intercomparison of two hydroxyl radical measurement techniques at the atmosphere simulation chamber SAPHIR, *J. Atmos. Chem.*, 56, 187–205, 2007.
- Schlosser, E., Brauers, T., Dorn, H.-P., Fuchs, H., Häsel, R., Hofzumahaus, A., Holland, F., Wahner, A., Kanaya, Y., Kajii, Y., Miyamoto, K., Nishida, S., Watanabe, K., Yoshino, A., Kubistin, D., Martinez, M., Rudolf, M., Harder, H., Berresheim, H., Elste, T., Plass-Dülmer, C., Stange, G., and Schurath, U.: Technical Note: Formal blind intercomparison of OH measurements: results from the international campaign HO<sub>x</sub>Comp, *Atmos. Chem. Phys.*, 9, 7923–7948, doi:10.5194/acp-9-7923-2009, 2009.
- Stevens, P. S., Mather, J. H., and Brune, W. H.: Measurement of tropospheric OH and HO<sub>2</sub> by laser-induced fluorescence at low pressure, *J. Geophys. Res.*, 99, 3543–3557, 1994.
- Tan, D., Faloona, I., Simpas, J. B., Brune, W., Shepson, P. B., Couch, T. L., Sumner, A. L., Carroll, M. A., Thornberry, T., Apel, E., Riemer, D., and Stockwell, W.: HO<sub>x</sub> budgets in a deciduous forest: Results from the PROPHET summer 1998 campaign, *J. Geophys. Res.*, 106, 24407–24427, 2001.
- Tanner, D., Jefferson, A., and Eisele, F.: Selected ion chemical ionization mass spectrometric measurement of OH, *J. Geophys. Res.*, 102, 6415–6425, 1997.
- Whalley, L. K., Edwards, P. M., Furneaux, K. L., Goddard, A., Ingham, T., Evans, M. J., Stone, D., Hopkins, J. R., Jones, C. E., Karunaharan, A., Lee, J. D., Lewis, A. C., Monks, P. S., Moller, S. J., and Heard, D. E.: Quantifying the magnitude of a missing hydroxyl radical source in a tropical rainforest, *Atmos. Chem. Phys.*, 11, 7223–7233, doi:10.5194/acp-11-7223-2011, 2011.